Hybrid Organic−Inorganic Xerogel Access to Meso- and Microporous Silica by Thermal and Chemical Treatment

Bruno Boury,[†] Pierre Chevalier,[†] Robert J. P. Corriu,*[,†] Pierre Delord,[‡] Joel J. E. Moreau,[§] and Michel Wong Chiman[§]

Laboratoire de Chimie Moléculaire et Organization du Solide, UMR 5637, and Groupe de Dynamique des Phases Condensées, UMR 5581, Université Montpellier II, Place E.Bataillon, 34095 Montpellier Cedex 5, France; and Laboratoire de Chimie Organométallique, ESA 5076, Ecole Nationale Supérieure de Chimie, 8 rue de l'Ecole Normale 34296 Montpellier Cedex 5, France

Received July 22, 1998. Revised Manuscript Received October 29, 1998

Hybrid xerogels of general formula $(O)_{1,5}Si-C\equiv C-(CH_2)_n-C\equiv C-Si(O)_{1,5}$ were prepared by sol−gel polycondensation in THF of the corresponding precursors $(H_3CO)_3Si-C\equiv C-(CH_2)_n-C\equiv C-Si(OCH_3)_3$, without catalyst. Treatment of the hybrid xerogels was with methanol and water in the presence of 2.0% of ammonium fluoride as catalyst. For $2 < n < 4$, elimination of the organic spacer was quantitatively achieved and the organic spacer was recovered in high yield. For $n = 5$, 6, and 8, increasing the length of the spacer results in a decreasing efficiency of this chemical treatment. Thermal oxidation at 600−680 °C of the hybrid xerogels was also performed and elimination of the organic spacer was obtained in all the cases. Mesoporous silica with a narrow pore-size distribution was obtained by chemical treatment of the xerogel with $n = 2-4$. Microporous silica was obtained by thermal treatment of the xerogel at 680 °C. All the materials were characterized by SAXS, BET, and spectroscopy analysis.

Introduction

Materials with tailor-made pore size and shape are potentially useful as nano- or subnanosized vessels, composites, or hosts for reaction and catalysis that require molecular imprinting.[1−3] Among the different way to achieve the engineering of porous silica-based materials, hybrid xerogels are receiving much attention since they can be prepared by the convenient sol−gel process.[4,5]

For example, nanocomposite hybrid materials were prepared by hydrolysis of a silica precursor (TMOS or TEOS) in the presence of dendrimers,[6] polymers,[7] or liquid crystals[8] as organic templates. The removal of the template then led to porous oxide. However, phase separation in organic−inorganic silica sols can diminish the homogeneity, and organic templating of amorphous silica could be best achieved from a homogeneous, molecularly defined, hybrid network in which the temporary organic templates are covalently bounded to a silica precursor. Such materials can be obtained by sol−gel hydrolysis of precursors containing nonhydrolyzable silicon−carbon bond like $R'Si(OR)_3$ or polysilylated $(RO)_3Si-Y-Si(OR)_3$.[9−11] Elimination of the organic fragment was generally achieved by oxidation reaction at high temperature. However, the thermal treatment and the heat generated by the combustion can promote structural relaxation and open up the walls of the existing pores to form mesoporous silica.[5]

We recently report how chemistry can be used, by removing the organic group of an hybrid xerogel under mild reaction conditions. Using $(O)_{1,5}Si-C\equiv C-(C_6H_4)-C\equiv C-Si(O)_{1,5}$ as precursor, cleavage of the $Si-C_{sp}$ bond was obtained by treatment with methanol and water in the presence of 2.0% of ammonium fluoride as catalyst.[12−15] This nonsacrificial route allowed preparation of a mesoporous silica and recovery of the organic spacer in high yield. The material thus obtained was a

[†] Laboratoire de Chimie Moléculaire et Organization du Solide, UMR 5637, Université Montpellier II.

[‡] Groupe de Dynamique des Phases Condensées, UMR 5581, Université Montpellier II.

[§] Ecole Nationale Supérieure de Chimie.

(1) Roger, C.; Hampden-Smith, M. J.; Brinker, C. J. *J. Mater. Res. Symp. Proc.* **1992**, *271,* 51.
(2) Lu, Y.; Cao, G. Z.; Kale, R. P.; Delattre, L. L.; Brinker, C. J. *J. Mater. Res. Symp. Proc.* **1996**, *435*, 271.
(3) Loy, D. A.; Buss, R. J.; Assink, R. A.; Shea, K. J.; Oiviatt, H. *Polym. Prepar. Am. Chem. Soc. Div. Polym. Chem.* **1993**, *34*, 244
(4) Sanchez, C.; Ribot, F. *New J. Chem.* **1994**, *18 (special issue).*
(5) Raman, K. N.; Anderson, M. T.; Brinker, C. J. *Chem. Mater.* **1996**, *8*, 1682.
(6) Chujo, Y.; Matsuki, S.; Kure, T.; Saegusu, T.; Yazawa, T. *J. Chem. Soc., Chem. Commun.* **1994**, 635.
(7) Antonietti, M.; Berton, B.; Goltner, C.; Hentze, H. P. *Adv. Mater.* **1998**, *10*, 155.
(8) Attard, G. S.; Glyde, J. C.; Goeltner, C. G. *Nature* **1995**, *378*, 366.
(9) Baney, R. H.; Itoh, M.; Sakakibara, A.; Suzuki, T. *Chem. Rev.* **1995**, *95*, 1410.
(10) Loy, D. A.; Shea, K. J. *Chem. Rev.* **1995**, *95*, 1431.
(11) Corriu, R. J. P.; Leclercq, D. *Angew. Chem., Int. Ed. Engl.* **1996**, *35*, 5.
(12) Chevalier, P.; Corriu, R. J. P.; Delord, P.; Moreau, J. J. E.; M., W. C. M. *New J. Chem.* **1998**, 423.
(13) Corriu, R. J. P.; Moreau, J. J. E.; Thépot, P.; Wong Chi Man, M. *Chem. Mater.* **1996**, *8*, 8.
(14) Corriu, R. J. P.; Moreau, J. J. E.; Thépot, P.; Wong Chi Man, M. *Chem. Mater.* **1992**, *4*, 1217.
(15) Corriu, R. J. P.; Moreau, J. J. E.; Thépot, P.; Wong Chi Man, M. *J. Sol-Gel Sci. Technol.* **1994**, *2*, 87.

10.1021/cm980519i CCC: $18.00
Published on Web 01/16/1999

mesoporous silica with a very narrow pore-size distribution that is stable upon calcination at 680 °C. An average pore diameter higher than the precursor's length was measured by BET measurement and confirmed by SAXS data. This difference was tentatively explained as the result of two factors, mainly the rearrangement of the silica occurring during the cleavage of the Si−C bond inducted by NH_4F as catalyst and also by the possible association of the precursor's molecules. In the same work, we have found that direct thermal oxidation of the hybrid xerogel at 600 °C resulted in a microporous silica with a broad pore-size distribution totally different from that of the one prepared by chemical treatment.

We studied the effect of the structure of the organic group by considering similar $(RO)_3Si-Y-Si(OR)_3$ compounds but with a polyconformational Y group instead of a rigid one like $C_2-C_6H_4-C_2$. Alkylene-bridged polysilsesquioxanes have been widely studied by Shea et al.;[16] however, the lack of reactivity of the Si−C bond in those precursors limited their use for chemical removal of the organic group, and we have chosen to prepare precursors of the general formula $(RO)_3Si-C\equiv C-(CH_2)_n-C\equiv C-Si(OR)_3$. A family of these compounds can be synthesized with increasing "flexibility". In this paper we compare the hybrid xerogels and their reactivity toward chemical and thermal treatment.

Results

1. Preparation of the Precursors. Precursors $\mathbf{P_{2-8}}$ with a spacer containing an alkyl bisethynyl unit were prepared following the general eq 1. The synthetic path

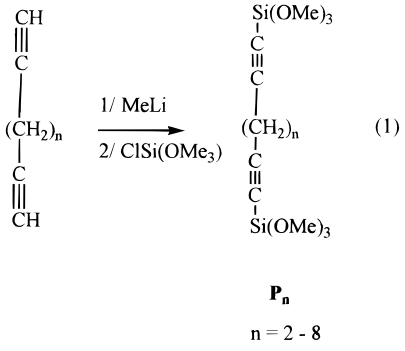

(1)

that we used can be applied to the preparation of all the precursors of this type: the metalation of the acetylenic H−C bond with MeLi generated a dilithium diacetylide, which was further reacted with $ClSi(OMe)_3$ and led to the functionalized bis(trimethoxysilyl) precursors $\mathbf{P_{2-8}}$. The compounds obtained in quantitative yield were purified by distillation; they were air and moisture sensitive and were fully characterized by spectroscopy analyses. [From a general point of view, in the present manuscript, the number used for the name of the compound and material refers to the number *n* used in the general formula $(RO)_3SiC\equiv C(CH_2)_nC\equiv CSi(OR)_3$.]

2. Preparation and Characterization of the Hybrid Xerogels. The hydrolysis and the condensation of precursors $\mathbf{P_{2-8}}$ were then performed under mild conditions in THF as polar and aprotic solvent by adding a stoichiometric amount of deionized water (pH = 6) at room temperature in the *absence of a catalyst* (eq 2).

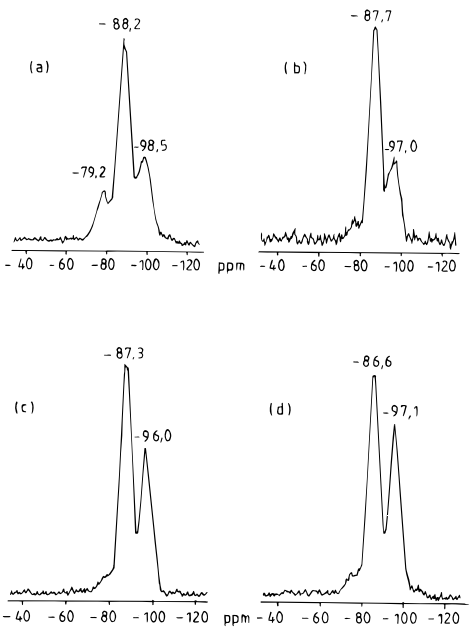

Figure 1. ^{29}Si CP MAS NMR spectra of hybrid xerogels of (a) $\mathbf{H_2}$, (b) $\mathbf{H_4}$, (c) $\mathbf{H_6}$, and (d) $\mathbf{H_8}$.

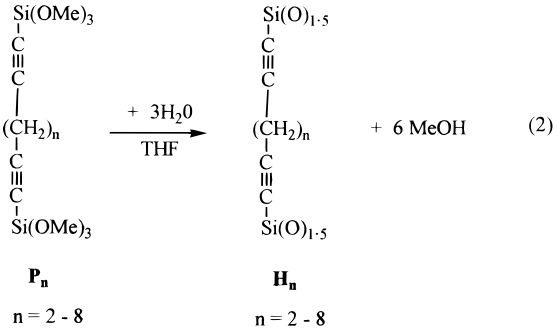

(2)

Gelation occurred within a few minutes, and the resulting gels were allowed to stand for aging 8 days for further condensation. They were then powdered, washed with solvents, and dried in a vacuum at room temperature.

All the collected hybrid xerogels, $\mathbf{H_{2-8}}$, were characterized by IR and NMR spectroscopy. Signals related to the presence of the organic spacer were observed by ^{13}C MAS NMR spectroscopy, between 19 and 29 ppm for alkyl carbon atoms and around 78 and 107 ppm for the two acetylenic carbon atoms. A signal at 51 ppm was attributed to a residual uncondensed methoxy group.

The signals observed by ^{29}Si CP MAS NMR analysis were characteristic of silicon atoms attached to three oxygen atoms and one sp carbon atom: T^1 $CSi(OR)_2(OSi)$ (R = Me or H) at −79 ppm; T^2 $CSi(OR)(OSi)_2$ (R = Me or H) at −87 ppm, and T^3 $CSi(OSi)_3$ at −95 ppm (Figure 1).[17] No signals corresponding to Q units were observed, indicating that cleavage of the Si−C bond during the hydrolysis of the precursors was avoided. From the qualitative NMR spectra the structure of the

(16) Oviatt, H. W.; Shea, K. J.; Small, J. H. *Chem. Mater.* **1993**, *5*, 3.

(17) Williams, E. A. *The Chemistry of Organic Silicon Compound*; Patai, S., Rappoport, Z., Eds.; Wiley: New York, 1989; p 511.

Scheme 1

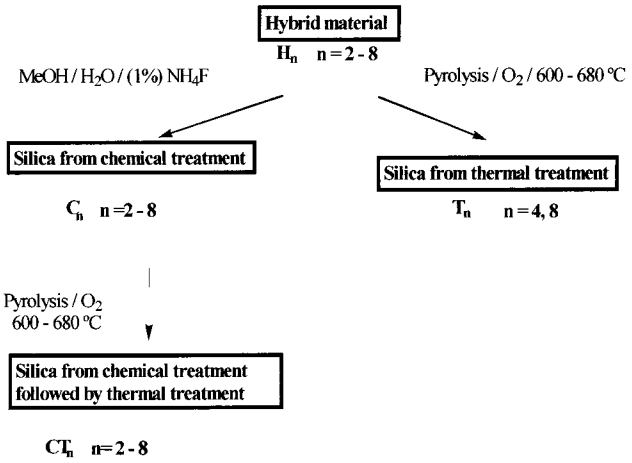

hybrid network can be described as siloxane chains with a bridging unit and with an average of one uncondensed OH or OMe group per silicon atom. Despite the essentially qualitative aspect of these measurements, comparison between these similar materials can be made. The percentages of each substructure were different, depending on the nature of the precursors. Both the increasing intensity of the signal of the T^3 units and the decreasing intensity of the T^0 units going from **H_2** to **H_8** indicated higher level of condensation in the latter case. This trend corresponds to an increase of the length and therefore of the flexibility of the spacer. It might be described in term of deformation of the precursors and mobility that allows the polycondensation between species initially far from each other. A similar trend was observed using bis(trialkoxysilyl)alkane precursors.[16]

3. Elimination of the Organic Fragment in the Hybrid Gels. Two different methods were investigated to eliminate the organic fragment: the mild hydrolytic cleavage of the Si−C bond in the presence of NH_4F as catalyst and the direct high-temperature air oxidation of the hybrid material (Scheme 1).

Mild Cleavage of the Si−C Bond. Removal of the organic spacer from the hybrid xerogel was performed by heating (65−70 °C) **H_{2-8}** for 4 days in MeOH and deionized water (pH = 6) in the presence of ammonium fluoride as catalyst (2.0%). Solid residues were extracted with pentane in order to separate the soluble organic compound from the insoluble silica residue **C_{2-8}**. Total removal of the organic spacer from the hybrid is depicted by eq 3. This reaction involving nucleophilic

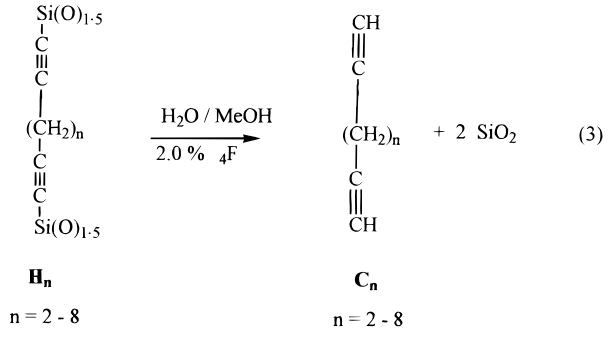

catalysis by fluoride ion is a well-documented process in organosilicon chemistry.[18,19]

Table 1. Formulation and Weight Loss of Silica Prepared by Chemical Treatment of Hybrid H_n ($2 < n < 8$)

silica residue	formulation	weight loss (%)
C_2	$C_{0.88}H_{2.05}O_{2.44}Si$	4−6
C_3	$C_{0.39}H_{1.12}O_{2.19}Si$	4−6
C_4	$C_{0.33}H_{0.93}O_{2.21}Si$	4−6
C_5	$C_{1.66}H_{2.55}O_{2.07}Si$	26
C_6	$C_{3.68}H_{4.92}O_{2.03}Si$	41
C_8	$C_{5.75}H_{8.33}O_{1.47}Si$	54.6

[a] Deduced from elemental analyses. [b] TG at 600 °C in dry air (flow rate of 40 mL min^{-1}).

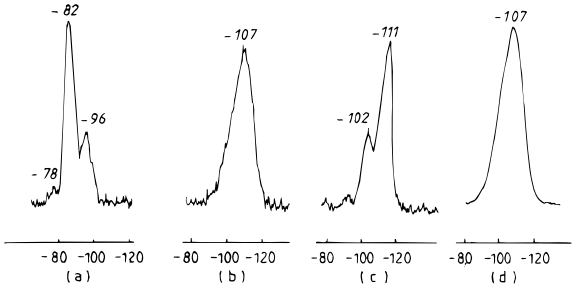

Figure 2. ^{29}Si CP MAS NMR spectra of (a) **H_4**, (b) **CT_4**, (c) **C_4**, and (d) **T_4**.

For **H_{2-4}**, the corresponding silica residues **C_{2-4}** contained low quantities of carbon (1 to 5%) measured by elemental analysis and corresponding to some residual spacers and nonhydrolyzed methoxy groups (Table 1). In these cases, the organic spacer was recovered in high yield (80−90% before purification). By ^{13}C NMR analyses, after long accumulation (10 000 scans), tiny signals corresponding to acetylenic and alky carbon atoms were observed. A signal at 85 ppm was attributed to acetylenic carbon C≡*C*−H. The ^{29}Si NMR spectrum of **C_4** exhibited resonances for mainly Q^3 *Si*(OH)$(OSi)_3$ at −102 ppm and a majority of Q^4 *Si*$(OSi)_4$ at −111 ppm (Figure 2). These spectroscopic data are consistent with the quantitative cleavage of the Si−C bond in the hybrids **H_{2-4}**, elimination of the organic moiety, and further condensation in the material to form new Si−O−Si linkages.

For **H_{5-8}**, the high carbon content in the corresponding silica residues **C_{5-8}** in addition to the low yield of recovered spacer indicated that elimination was only partial in these cases. The signals observed at 107, 77, and 19−29 ppm by ^{13}C NMR analyses of residues **C_{5-8}** are consistent with the presence of the organic spacer. An additional signal at 85 ppm was attributed to acetylenic carbon C≡*C*−H. It indicates that cleavage of one of the Si−C links has occurred, leading to a spacer linked to the silica matrix by one Si−C bond. Interpretation of the ^{29}Si NMR data was limited because a set of broad signals was observed, corresponding to T^2 (−87 ppm), T^3 (−96 ppm), Q^1 (−86 ppm), Q^2 (−93 ppm), Q^3 (−101 ppm), and Q^4 at (−109 ppm). The presence of these entities arose from the partial cleavage of the Si−C bond. Qualitatively, the signal intensity of each of the Q^n substructure increases with the percentage of removed organic spacer.

The thermogravimetry analyses of **C_{2-8}** were performed at 600−680 °C in dry air. In all the case, this

(18) Kuwajima, I.; Nakamura, E.; Hashimoto, K. *Tetrahedron* **1983**, *39*, 975.
(19) Corriu, R. J. P.; Gerin, C.; Moreau, J. J. E. *Top. Curr. Chem.* **1984**, *15*, 43.

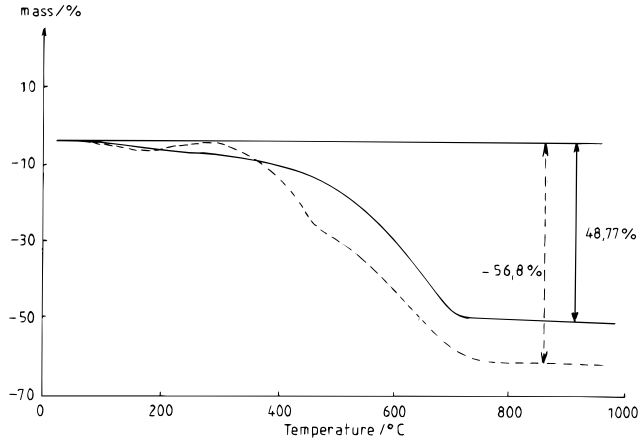

Figure 3. TG curve of (a) $\mathbf{H_4}$ and (b) $\mathbf{H_8}$.

postcalcination treatment led to a limited mass loss of 4−6% observed before 200 °C and arising, first, from the elimination of water absorbed by the material and, second, from the formation of methanol produced by further condensation of the residual Si−OH and Si−OMe functions. Between 200 and 680 °C, oxidative elimination of the organic resulted in a mass loss of various intensity, depending on the starting $\mathbf{C}_n$ material. According to these analyses, less than 5% of residual spacer was present in $\mathbf{CT_{2,3}}$, and about 10% in $\mathbf{CT_4}$, 60% in $\mathbf{CT_5}$, 85% in $\mathbf{CT_6}$, and 100% in $\mathbf{CT_8}$.

Removal of all the residual organic spacers was obtained by thermal treatment of $\mathbf{C_{2-8}}$ under the same conditions as used for TG analysis (Scheme 1). $\mathbf{CT_{2-8}}$ were obtained and characterized as carbon free silica by elemental analyses and ^{29}Si CP MASS NMR spectroscopy, which exhibited one signal centered at −108 ppm, consistent with the presence of Q,[4] Q^3, and Q^2 substructure, as exemplified by $\mathbf{CT_4}$ in Figure 2.

High-Temperature Oxidation of the Organic Template. Removal of the organic spacer was also achieved by directly heating the hybrid material up to 680 °C in air for 3−4 h (Scheme 1); this reaction formally corresponds to eq 4 and was carried out on $\mathbf{H_4}$ and $\mathbf{H_8}$ to obtain to

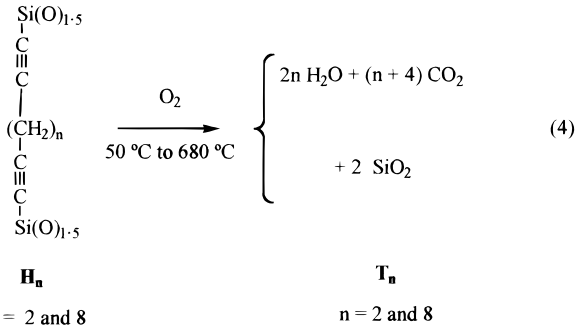

(4)

silica $\mathbf{T_{4-8}}$. In Figure 3 is presented the TG curve of $\mathbf{H_4}$ and $\mathbf{H_8}$, and the limited mass loss of 4−3% observed before 300 °C corresponds to the elimination of compounds absorbed in the hybrid material or produced by further condensation of the residual functions. Between 200 and 680 °C an important mass loss, close to the theoretical one, arises from the oxidative elimination of the organic spacer: 56.8% for $\mathbf{H_8}$ (theoretical, 57%) and 48.7% for $\mathbf{H_4}$ (theoretical, 45%). Using this sacrificial route, pure free-carbon silica was produced in both cases. Solid-state ^{29}Si NMR analyses of $\mathbf{T_4}$ and $\mathbf{T_8}$ show

Table 2. Surface and Porosity Properties of $\mathbf{H}_n$, $\mathbf{C}_n$, and $\mathbf{CT}_n$ Material ($2 \le n \le 8$)

	specific surf. area ($m^2\ g^{-1}$)	pore volume ($cm^3\ g^{-1}$)	pore diam (Å)	Si−C≡C−$(CH_2)_n$−C≡C−Si distance[a] (Å)
$\mathbf{H_2}$	360			6.0
$\mathbf{C_2}$	935	0.64	27.6	
$\mathbf{CT_2}$	780	0.48	24.8	
$\mathbf{H_3}$	<10			6.9
$\mathbf{C_3}$	684	0.88	51.3	
$\mathbf{CT_3}$	685	0.85	49.5	
$\mathbf{H_4}$	<10			8.4
$\mathbf{C_4}$	441	0.78	70.4	
$\mathbf{Ct_4}$	407	0.72	70.5	
$\mathbf{T_4}$	345	0.17		
$\mathbf{H_5}$	<10			9.4
C_5	383	0.36	38.0	
CT_5	516	0.44	34.2	
$\mathbf{H_6}$	<10			10.9
$\mathbf{C_6}$	58	0.09	62.2	
$\mathbf{CT_6}$	329	0.20	24.9	
$\mathbf{H_8}$	<10			13.3
$\mathbf{C_8}$	<10			
$\mathbf{CT_8}$	298	0.13	15.1	
$\mathbf{T_8}$	96	0.04	<5	

[a] Determined by computer simulation using Cerius[2] simulation program.

a broad signal centered at −108 ppm attributed to Q,[4] Q^3, and Q^2 substructure units (Figure 2), the presence of Q^2 and Q^3 being confirmed by infrared band absorption corresponding to Si−OH (νSi−OH, 3451 cm^{-1}).[20]

4. Morphological Feature and Surface Area of the Xerogels before and after Treatment. *Gas sorption porosimetry* was selected to evaluate the specific surface area and the pore structure of the different materials.[21,22] With the exception of $\mathbf{H_2}$, all the hybrid materials have a low specific surface area (<10 $m^2\ g^{-1}$), according to BET experiments using nitrogen adsorption (Table 2), independent of the length of the spacer. Similar behaviors were reported by Shea et al. using bis(trialkoxysilyl)alkane monomers and acid−base conditions.[16] The high surface area observed for $\mathbf{H_2}$ is probably related to the rigidity of the spacer, and a similar result was reported for another rigid-rod organic group.[14,23]

The formation of a porous material from a nonporous hybrid xerogel was clearly related to the efficiency of the chemical treatment for removing the organic part: $\mathbf{H_{2-5}}$ gave porous material $\mathbf{C_{2-5}}$, while $\mathbf{H_{6,8}}$ gave no porous materials $\mathbf{C_{6,8}}$ (Table 2). For example, a type IV isotherm adsorption−desorption plot is observed for $\mathbf{C_{2-5}}$ with a type H1 and H2 hysteresis loop (type E in de Boer classification) (Figure 4).[21] It suggests the presence of cylindrical-shaped pores or an ink bottle, by reference to a similar isotherm of silica gel. Using the BJH model,[24] the cumulative pore volume plot gives information regarding the pore-size distribution. For each of the materials, the dV/d(log D) curve shows a different proportion of micropores (<20 Å) and of

(20) Colthup, N. B.; Daly, C. H.; Wiberley, S. E. *Introduction to Infrared and Raman Spectroscopy*; Academic Press: London, 1990.
(21) Gregg, S. J.; Sing, K. S. W. *Adsorption Surface Area and Porosity*, 2nd ed.; Academic Press: London, 1982.
(22) Lowell, S.; Shields, J. E. *Powder Syrface Area and Porosity*, 2nd ed.; Chapman and Hall: London, 1984.
(23) Shea, K. J.; Loy, D. A.; Webster, O. W. *Chem. Mater.* **1989**, *1*, 572.
(24) Barrett, E. P.; Joyner, L.; Halenda, P. P. *J. Am. Chem. Soc.* **1951**, *73*, 373.

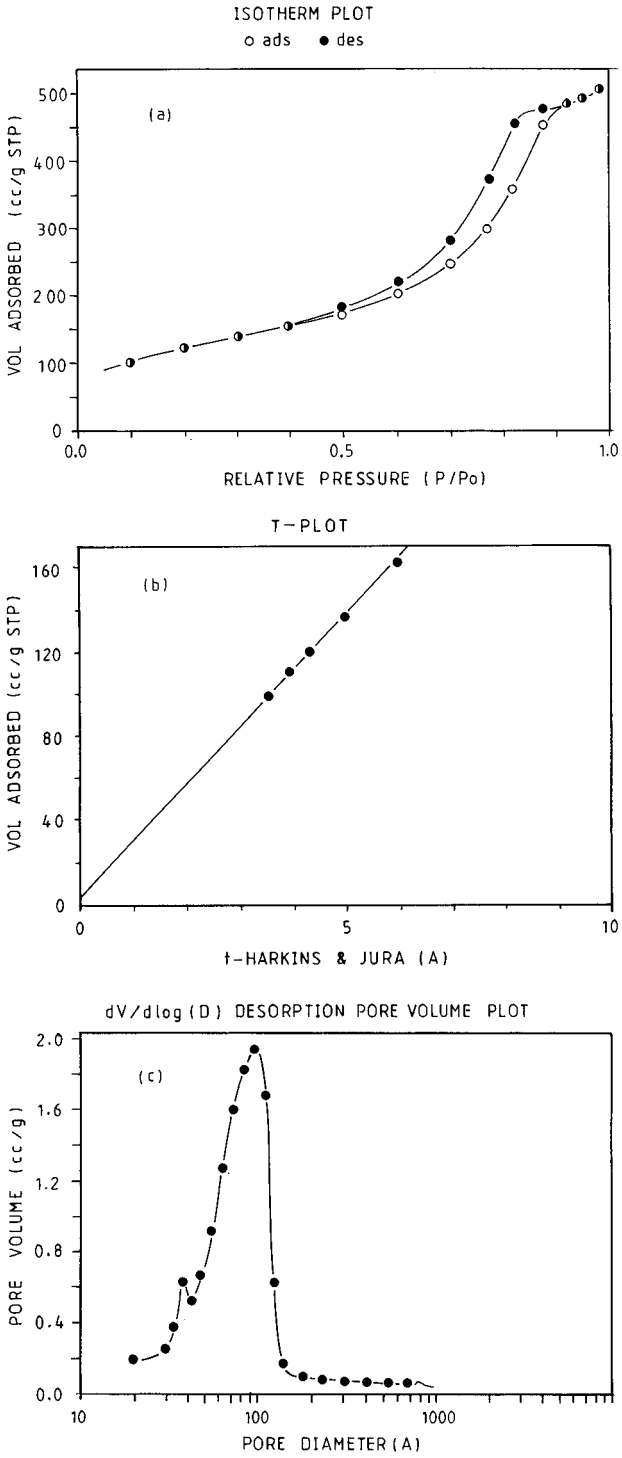

Figure 4. Isotherm plots (a), *t*-plot (b), and desorption pore volume plots (c) of $\mathbf{C_4}$.

mesopores (<200 Å) (Figure 5). For $\mathbf{C_2}$, we observed a high level of micropores and a rather narrow pore-size distribution centered at 36 Å. By the same analysis, $\mathbf{C_3}$ was characterized as a mesoporous material with a narrow pore-size distribution centered at 50 Å. For $\mathbf{C_4}$, $\mathbf{C_8}$, bidispersed narrow size distributions were observed along with different levels of micropores: at 40 and 100 Å for $\mathbf{C_4}$ and at 30 and 70 Å for $\mathbf{C_6}$ and at 40 and 85 Å for $\mathbf{C_8}$.

Further heating at 680 °C in air has different effects, depending on the texture and the composition of the material which depends on the initial efficiently of the chemical treatment. For $\mathbf{C_2}$ this treatment led to a decrease of the surface area (around 16%) and the proportion of micropores in the resulting $\mathbf{CT_2}$ material. The postcalcination of $\mathbf{C_{3,4}}$ did not modify the initial texture parameters, which were basically similar for the corresponding $\mathbf{CT_{3,4}}$.

A different behavior was observed for $\mathbf{C_{5-8}}$ since, upon oxidative thermal treatment, the residual organic spacer was eliminated and porosity generated. The resulting carbon-free silica $\mathbf{CT_{5-8}}$ presented a completely different pore-size distribution compared with the pore-size distribution obtained after chemical treatment. No clear trend emerged from these results since, in these cases, the effects of the chemical and the thermal treatment are combined due to the incomplete elimination of the organic units.

It was of interest to compare the pore structure of the above material $\mathbf{C_{4,8}}$ with that of the silica $\mathbf{T_{4,8}}$ prepared by direct oxidation of $\mathbf{H_{4,8}}$ at high temperature in oxygen flow. We focused on the study of $\mathbf{H_4}$ and $\mathbf{H_8}$ because they presented completely different behaviors toward chemical treatment. By BET measurement of $\mathbf{T_4}$ and $\mathbf{T_8}$ we did not observed any narrow pore-size distribution, and thermal treatment of these two hybrids resulted in similar microporous carbon-free silica (Figure 6). For both materials, an isotherm of type I and *t*-plot curves were representative of a highly microporous material with an important proportion of ultramicropores (<5 Å).

Small angle scattering of X-rays (SAXS) is sensitive to the fluctuations of electronic density in the medium.[12,25] Here, we focused on $\mathbf{H_4}$ and $\mathbf{H_8}$ and their related materials prepared by thermal or chemical treatment. These starting hybrid xerogels presented a very similar behavior: the small angle scattering intensity decreased continuously between 2×10^{-3} and 0.1 Å^{-1}. A powerlaw, respectively in $q^{-2.5}$ and q^{-3} for $\mathbf{H_4}$ and $\mathbf{H_8}$, represents correctly the intensity comportment between 5×10^{-3} and 1×10^{-1} Å^{-1} (Figures 7 and 8) and a fractal behavior might be assumed. Meanwhile the differences observed between the two xerogels are not understood at the present time; more work is needed to fully described their respective structure.

For the mesoporous silica $\mathbf{C_4}$ obtained by chemical treatment of $\mathbf{H_4}$, a q^{-4} slope of the spectrum was measured in the Porod region between 0.08 Å < q < 0.2 Å, indicating a smooth surface of the silica phase. A plot $\ln(qI)$ versus q^2 shows a linear behavior that allows determination of a pore diameter, assuming the pores are elongated cylinders. The diameter calculated, 60−64 Å, is in good agreement with the pore diameter measured by BET analysis, 70 Å (Table 2).

The spectra of $\mathbf{C_4}$ is quite similar to that of $\mathbf{CT_4}$ on the whole scanned domain. This is a good indication that pyrolysis at 680 °C of the material obtained after chemical removal of the organic fragment does not affect significantly the structure of the porous medium. A similar result was reported when using a phenylene group as the spacer.[12]

The spectrum of $\mathbf{C_8}$ does not show a very different intensity curve that the one of $\mathbf{H_8}$. This is not surprising, since the removal of the organic group in $\mathbf{H_8}$ was not achieved by chemical treatment. There is only a broad shoulder on the $\mathbf{C_8}$ intensity, which is very difficult to

(25) Glatter, O.; Kratky, O. *Small Angle X-ray Scattering*; Academic Press: London, 1982.

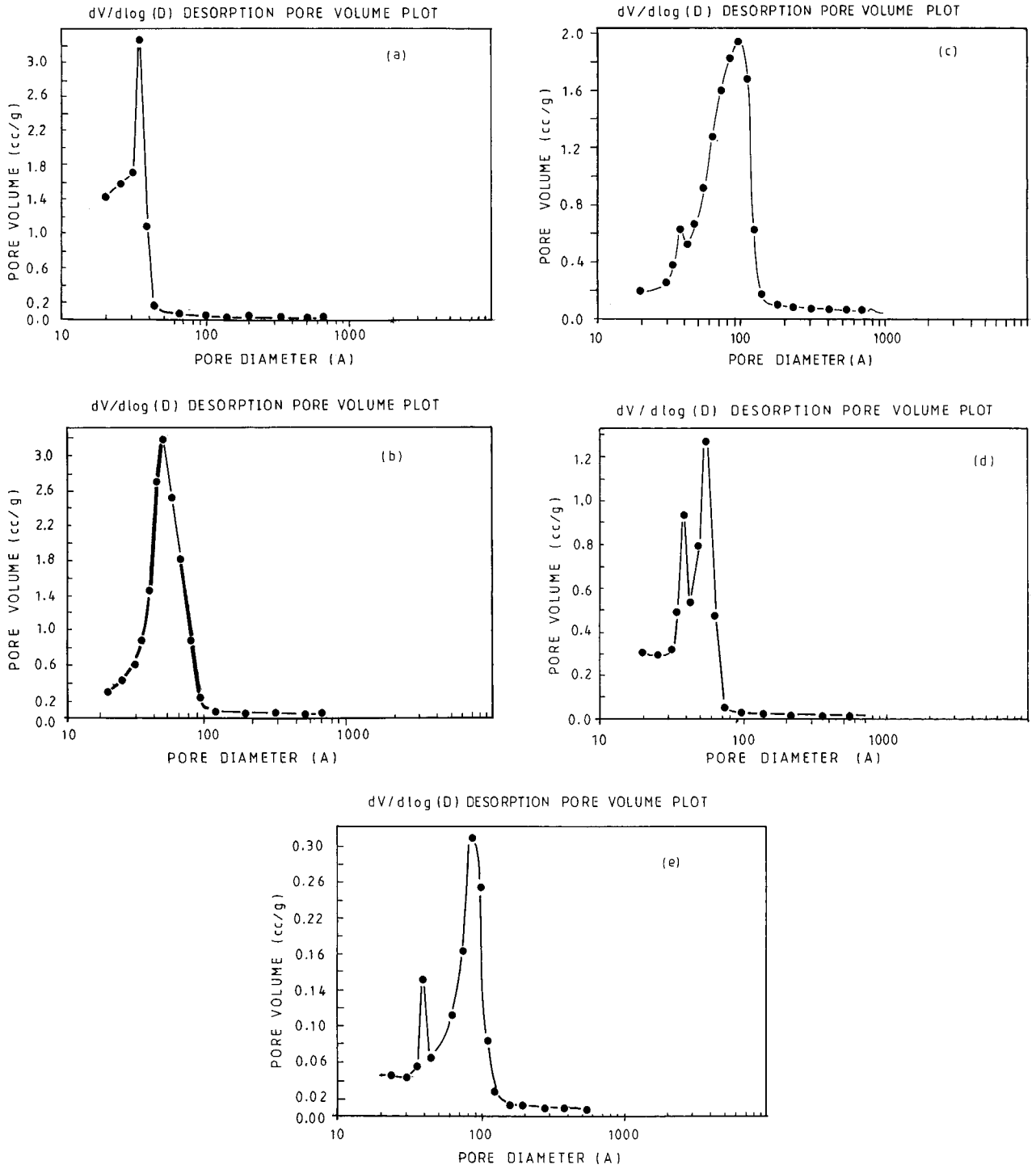

Figure 5. Desorption pore volume plots of (a) $\mathbf{C_2}$, (b) $\mathbf{C_3}$, (c) $\mathbf{C_4}$, (d) $\mathbf{C_5}$, and (e) $\mathbf{C_6}$ prepared by chemical treatment of the corresponding hybrid xerogels.

interpret at this time. However, it clearly reflects a structural modification of the material and confirms the elemental analysis on that point.

For silica $\mathbf{T_4}$ and $\mathbf{T_8}$ obtained by direct oxidation of the corresponding xerogel $\mathbf{H_4}$ and $\mathbf{H_8}$, the general pattern of the curves is similar to those of the starting hybrid xerogels; the higher intensity arises from a better contrast in these materials related to the formation of porosity.

Discussion

The organic template approach of the formation of silica with controlled pore size is currently under investigation.[5] Beside the templating route using micelles,[26,27] the hybrid materials approach is well-documented, since organic ligands (pendant,[28−30] bridging,[10,14] or polymerizable group[31,32]) have been incorporated in a silica matrix and can be subsequently

(26) Tanev, T. P.; Pinnavaia, T. J. *Science* **1995**, *267*, 865.
(27) Corma, A. *Chem. Rev.* **1997**, *6*, 22387.
(28) Chen, C. F.; Luan, Z.; Klinowski, J. *Langmuir* **1995**, *11*, 2815.
(29) Liu, C.; Komarneni, S. *Mater. Res. Soc. Symp. Proc.* **1995**, 371.
(30) Schmidt, H.; Wolter, H. *J. Non-Cryst. Sol.* **1990**, *121*, 428.
(31) Delattre, L.; Dupuy, C.; Babonneau, F. *J. Sol-Gel Sci. Technol.* **1994**, *2*, 185.
(32) Yanagisawa, T.; Shimizu, T.; Kuroda, C. *Bull. Chem. Soc. Jpn.* **1990**, *63*, 988.

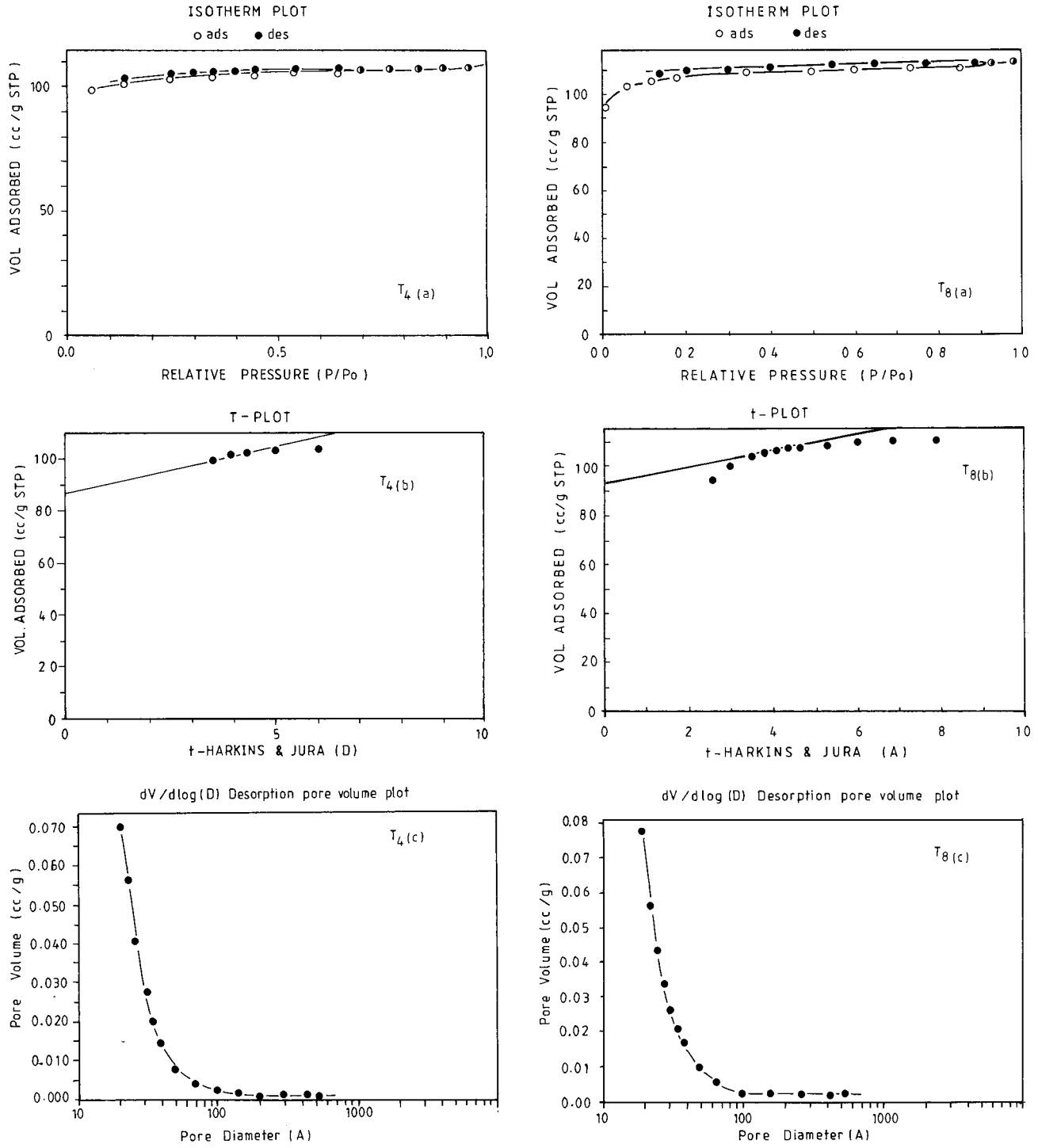

Figure 6. Isotherm plots (a), *t*-plot (b), and desorption pore volume plots (c) of $\mathbf{T_4}$ and $\mathbf{T_8}$.

removed. The present work is based on hybrid xerogels that are formed by sol−gel uncatalyzed hydrolysis of $(MeO)_3Si-C\equiv C-(CH_2)_n-C\equiv C-Si(OMe)_3$.

The presence of the Si−C≡C group allows the elimination of the organic group under mild, catalyzed conditions. This reaction, catalyzed by fluoride ion, involves nucleophilic attack of H_2O on a pentacoordinated silicon atom.[12,19,32,33] It leads to Si−C bond cleavage and formation of Si−OH groups that can further polycondense either between each other or by reacting with residual Si−OMe group. Therefore, such a step by step cleavage/condensation reaction, as depicted in Schemes 2 and 3, leads to the elimination of the organic acetylenic molecule and generates a silica network.

Efficiency of This Chemical Treatment. The present results show that the efficiency of this chemical treatment depends on the structure of the organic part of the precursor: chemical treatment is efficient on $\mathbf{H_{2-5}}$ while the organic part cannot be removed from $\mathbf{H_8}$. From a general point of view, the efficiency of the chemical treatment decreases upon increasing the length of the

(33) Corriu, R. J. P.; Guerin, C. *J. Organomet. Chem.* **1980**, *198*, 231.

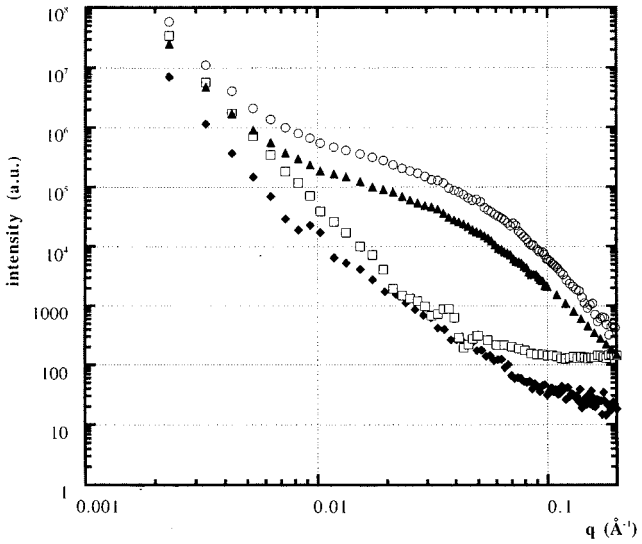

Figure 7. Intensity vs scattering vector q (log scale) for (◆) **H₄**, (○) **C₄**, (□) **CT₄**, and (▲) **T₄**.

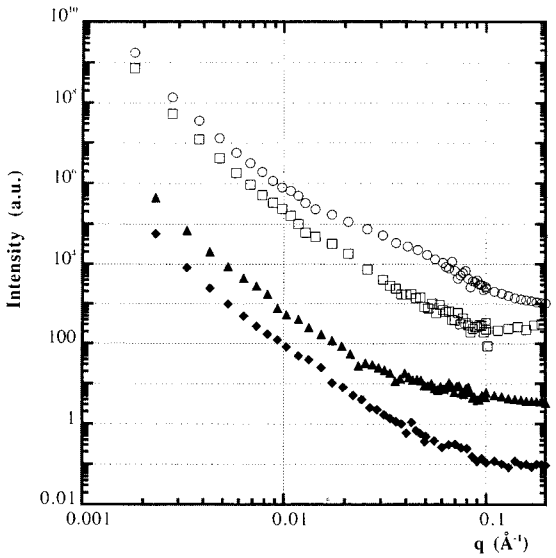

Figure 8. Intensity vs scattering vector q (log scale) for (◆) **H₈**, (○) **C₈**, (□) **CT₈**, and (▲) **T₈**.

spacer. This is not dependent on the surface area of the xerogel, since removal of the organic part was achieved for **H₂** (360 $m^2\ g^{-1}$) and **H₃₋₅** (<10 $m^2\ g^{-1}$). Similarly, elimination of the organic group by chemical treatment of nonporous xerogels with a $-C{\equiv}C-C_6H_4-C{\equiv}C-$ spacer was quantitatively achieved under the same conditions.[12] The structure, particularly the rigidity, of the spacer appears as the major parameter that governs its reactivity in the present case. Apparently, the ability of chemical treatment to remove the organic group is related to the accessibility of the reagent to the $Si-C{\equiv}$ bonds in the xerogel and is certainly also related to the level of condensation, since the increasing intensity of the T^3 signal is observed from **H₂** to **H₈**. In addition to the steric effect, the efficiency might also result from the balance of hydrophobic and hydrophilic interaction. Indeed, this chemical treatment is carried out in a very polar medium ($MeOH/H_2O$), and increasing the length of the organic spacer increases the hydrophobic character of the solid, which can prevent access of the reagent to the $Si-C{\equiv}$ bond.

For **H₂₋₄**, complete removal of the organic part was achieved and it is noteworthy that the pore size is much larger than the size of the organic molecule which is eliminated (Table 2). Meanwhile, the pore structure is quite homogeneous in size in all cases, and the average pore diameter decreases as the size of the organic fragment in the hybrid network decreased. The same trend was observed for $O_{1.5}Si-C{\equiv}C-C_6H_4-C{\equiv}C-SiO_{1.5}$ xerogels.[12] However, compared to the silica obtained from chemical treatment of $O_{1.5}Si-C{\equiv}C-(CH_2)_n-C{\equiv}C-SiO_{1.5}$ ($n = 2, 3, 4$) xerogels, the silica obtained upon chemical treatment of the $O_{1.5}Si-C{\equiv}C-C_6H_4-C{\equiv}C-SiO_1$ xerogel exhibits a much more narrow pore-size distribution (50−60 Å). Therefore, there is apparently a relation between the pore structure and the nature of the organic bridging spacer.

Effect of the Chemical Treatment. The discrepancy between spacer and pore size could result from an association of the spacer occurring during the polycondensation step. Each of the organic spacer is always covalently linked to the siloxane network since ^{29}Si NMR exhibits only T units without any Q units. Thus, the formation of a siloxane phase domain and organic domain can be considered only at a nanosize level.[11] The structural organization of these materials is currently under investigation in our laboratory. Whatever the organization of the spacer is, all of them are necessarily close to each other, since we do not use any dilution with silica precursors such as TMOS. Therefore, the void left by their elimination upon chemical treatment is connected and can result in a pore size exceeding the spacer size by a percolation process.

It can also be assumed that the growing and rearrangement of the resulting silica network takes place at the interface between the solution and the solid. Simultaneously to the cleavage of the Si−C bonds, formation of Si−OH group can lead to further condensation. The rearrangement of the silica network is also evidenced by the NMR data; the production of mainly Q^3 and Q^4 units from a starting hybrid xerogel with T^3 and T^2 units corresponds obviously to an increase of the level of condensation which cannot be explained by the cleavage of the $Si-C_{sp}$ bond. A reorganization of the silica network induced and nucleophilically caltalyzed by F^- is occurring, as proposed in our previous works.[12] However, the homogeneity of the pore structure is clearly observed experimentally. This phenomena is not well-understood at this time but it might be related to the homogeneous dispersion of the organic group at the molecular level in the starting hybrid material.

Effect of the Thermal Treatment after Chemical Treatment. The stiffness of the silica network obtained after chemical treatment is not equivalent for all the materials. For example, the mesoporous silica network of **C₃** and **C₄** is strong enough to withstand a thermal treatment at 680 °C under oxygen, and no modification of the pore-size diameter or the specific surface area is observed before and after thermal treatment. For **C₂**, a decrease of the pore diameter and the specific surface area is observed and is certainly promoted by a sintering phenomena, with loss of hydroxyls and structural relaxation resulting in densification of the silica net-

Scheme 2

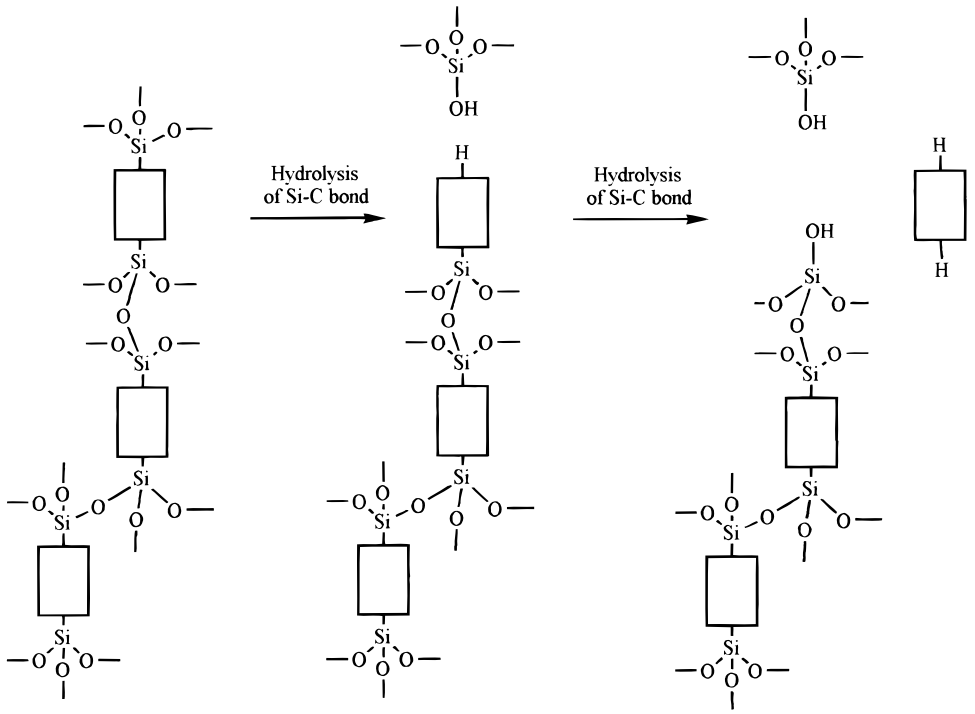

Scheme 3

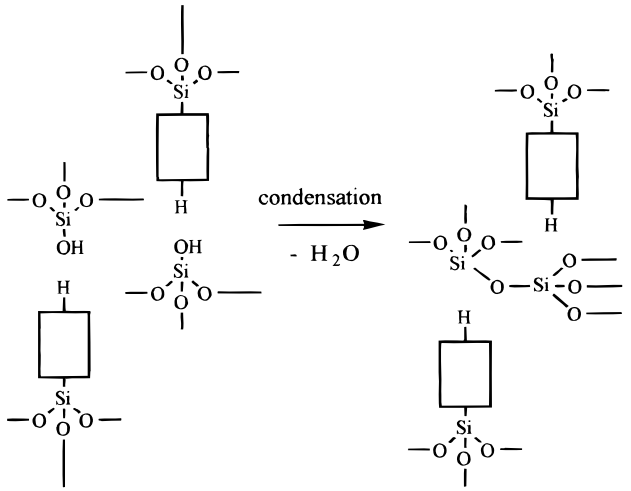

work.[34] Such a difference can be related to the high level of micropores in **C₂**, while for **C₃** and **C₄** the rearrangement of the silica produced certainly a stronger network with larger pore size (mesoporous material), so no sintering/relaxation occurs on heating.

Thermal Treatment of the Hybrid. The silica **C₄** resulting from the chemical treatment is completely different from that of the silica **T₄** produced by oxidation at high temperature. This treatment efficiently removed the organic group in all the cases. For both the **C₄** and **C₈** systems, the stress generated during the thermal treatment and the thinness of the initial silica network could have result in its partial collapse, in agreement with the criteria proposed by Brinker et al. on the role of covalently bonded template ligands in pore-size direction for this type of hybrid material.[5] However, in the present case, we note that the SAXS curves of the couples **H₄**/**T₄** and **H₈**/**T₈** present some similarity. The sum of these results can be interpreted in terms of a better "conservation" of the silica network in the case of thermal treatment. At the contrary, a total rearrangement of the silica network during the chemical treatment is observed.

Conclusion

The present results point out that the reactivity of polysilsesquioxanes xerogels of general formula $(O)_{1,5}Si-C\equiv C-(CH_2)_n-C\equiv C-Si(O)_{1,5}$ depends on the nature of the spacer. For short polyalkylene groups, with $n = 2-4$, the spacer can be remove and a mesoporous silica is obtained with a narrow pore-size distribution. In that case, the pore diameter increases with the size of the organic spacer, meanwhile it is always higher than the size of the organic spacer; this behavior is similar to that of hybrid xerogels with a rigid spacer like a phenyl group, which we already reported. For a long group, *n* being equal to 5, 6, and 8, the ability to remove the organic spacer deacreases with the length of the spacer.

In all the cases the oxidative thermal treatment leads to microporous silica with a broad pore-size distribution completely different from the silica obtained by chemical treatment. In this last case, the final texture of the silica result apparently of the simultaneous cleavage of the $Si-C_{sp}$ bond and a rearrengement of the Si−O−Si network. The elucidation of such behavior requires more investigations on the structure of these hybrid xerogels, particularly on the organization of the organic groups within the materials.

Experimental Section

All reactions were carried out under nitrogen by use of a vacuum line and Schlenk tube techniques. Solvents were dried and distilled before use. Melting points were determined with

(34) Brinker, C. J.; Scherer, G. W. *Sol−Gel Science*; Academic Press Inc.: Boston, 1990.

a Gallenkamp apparatus and are uncorrected. IR spectra were recorded by using a Perkin-Elmer 1600 FTIR spectrometer. ^{1}H NMR spectra were recorded on a Bruker AW 80 and Bruker AC 250 spectrometer, and ^{13}C and ^{29}Si NMR spectra were recorded both in solution and in the solid state on a Bruker WP 250 FT AM300 apparatus. Solvents and chemical shifts (δ relative to Me_4Si) are indicated. Mass spectra were measured on a JEOL JMS-DX 300 mass spectrometer (ionization energy 70 eV).

Thermogravimetric and differential analysis (TGA−TDA) were performed under flowing air (50 mL min^{-1}) with a Netzsch STA 409 thermobalance, the typical heating rate being 10 °C min^{-1}. The pyrolysis experiments were performed under dry air with a tubular Carbolite furnace with internal Eurotherm programming and were carried out by pouring weighed samples of solids into an aluminum oxide boat placed in an aluminum oxide tube connected to a vacuum line. Gas flow was maintained around 50 mL min^{-1} during pyrolysis. The surface areas, pore volume, and the pore-size distribution were determined by analyzing the N_2 adsorption/desorption isotherms according to the BET method using a Micromeritic ASAP 2400 apparatus. X-ray powder diffraction measurements were performed using a Seifert M24 apparatus. Elemental analysis were carried out by the "Service Central de Microanalysis du CNRS". The photographs of solids were collected by transmission electro micrography (TEM) using a JEM 1200 EX2 apparatus. SAXS experiments were carried out on a high-resolution Bonse-Hart camera with two germanium channel cuts[20] for very small q values [three reflections on (111) planes for each crystal] and on a low-resolution classical apparatus with a Ge(111) monochromator and a linear detector for q values >0.03 Å^{-1}. The wavelength is 1.542 Å (Cu Kα radiation) The specimen were powdered and dried samples. The spectra were dismayed with adapted procedures.

1,6-Bis(trimethoxysil)-1,5-hexadiyne, P_2. To a solution of 1,5-hexadiyne in pentane (50% weight) (11.0 g, 70.4 mmol) in tetrahydrofuran (350 mL) cooled at −50 °C is added dropwise, via an additional funnel, a solution of MeLi/LiBr in ether (110 mL, [MeLi] = 1.5 M) with stirring. The reaction mixture is then heated 2 h at room temperature and a yellowish suspension is obtained and is then cooled at −50 °C and poured dropwise via a metallic pipe to a solution of chlorotrimethoxysilane (26.5 g, 169 mmol) in 60 mL of THF kept at −70 °C. After addition, the reaction is stirred at room temperature for 4 h. Filtration of the solid and evaporation of the solvent gives a viscous greenish liquid. Distillation (99 °C, 2×10^{-2} mmHg) afforded 15.65 g (70% yield) of **P_2** as a pale yellow liquid. IR (CCl_4, ν cm^{-1}): 1140, 1430, 1461, 2191, 2848, 2938. ^{1}H NMR (CCl_4, δ, ppm): 2.32 (4H, s), 3.35 (18H, s). ^{13}C NMR ($CDCl_3$, δ, ppm): 19.38 (t), 50.69 (q), 76.26 (s), 104.90 (s). ^{29}Si NMR ($CDCl_3$, δ, ppm): −69.51. Mass spectrum (EI; *m/e*, relative intensity): 318 (4, M^+). Elemental analyses calculated for $C_{12}H_{22}O_6Si_2$: C, 45.26; H, 6.96. Found: C, 41.65; H 6.95.

1,7-Bis(trimethoxysil)-1,6-heptadiyne, P_3. An experimental procedure similar to that used for the preparation of **P_2** was used. The following quantities were used: 1,6-hexadiyne (9.5 g, 103.1 mmol) in tetrahydrofurane (350 mL); solution of MeLi/LiBr in ether (160 mL, [MeLi] = 1.5 M); chlorotrimethoxysilane (38.8 g, 247.4 mmol) in 80 mL of THF. Distillation (120 °C, 2×10^{-2} mmHg) gave 17.8 g (yield, 52%) of a pale yellow liquid. IR (CCl_4, ν cm^{-1}): 1090, 1429, 1455, 2185, 2839, 2941. ^{1}H NMR (CCl_4, δ, ppm): 1.75 (2H, q), 2.36 (4H, t), 3.51 (18H, s). ^{13}C NMR ($CDCl_3$, δ, ppm): 18.25 (t), 26.58 (t), 50.24 (q), 75.53 (s), 105.99 (s). ^{29}Si NMR ($CDCl_3$, δ, ppm): −69.58. Mass spectrum (EI; *m/e*, relative intensity): 332 (12, M^+). Elemental analyses calculated for $C_{13}H_{24}O6Si_2$: C, 46.96; H, 7.28. Found: C, 46.91; H 7.18.

1,8-Bis(trimethoxysil)-1,7-octadiyne, P_4. An experimental procedure similar to that used for the preparation of **P_2** was used. The following quantities were used: 1,7-octadiyne (8.2 g, 77.2 mmol) in tetrahydrofurane (350 mL); solution of MeLi/LiBr in ether (120 mL, [MeLi] = 1.5 M); chlorotrimethoxysilane (29.0 g, 185.4 mmol) in 100 mL of THF. Distillation (129−135 °C, 2×10^{-2} mmHg) gave 17.6 g (yield, 66%) of a pale yellow liquid. IR (CCl_4, ν cm^{-1}): 1086, 1428, 1460, 2185, 2843, 2943. ^{1}H NMR (CCl_4, δ, ppm): 1.47 (4H, q), 2.09 (4H, t), 3.29 (18H, s). ^{13}C NMR ($CDCl_3$, δ, ppm): 19.36 (t), 27.39 (t), 51.02 (q), 75.32 (s), 107.59 (s). ^{29}Si NMR ($CDCl_3$, δ, ppm): −69.26. Mass spectrum (EI; *m/e*, relative intensity): 346 (1, M^+). Elemental analyses calculated for $C_{14}H_{26}O6Si_2$: C, 48.53; H, 7.56. Found: C, 47.09; H 7.16.

1,9-Bis(trimethoxysil)-1,8-nonadiyne, P_5. An experimental procedure similar to that used for the preparation of **P_2** was used. The following quantities were used: 1,8-nonadiyne (14.7 g, 122.3 mmol) in tetrahydrofurane (400 mL); solution of MeLi/LiBr in ether (190 mL, [MeLi] = 1.5 M); chlorotrimethoxysilane (46.0 g, 293.5 mmol) in 100 mL of THF. Distillation (138−140 °C, 2×10^{-2} mmHg) gave 35.1 g (yield, 80%) of a pale yellow liquid. IR (CCl_4, ν cm^{-1}): 1181, 1428, 1463, 2188, 2847, 2925. ^{1}H NMR (CCl_4, δ, ppm): 1.33 (6H, m), 2.05 (4H, t), 3.31 (18H, s). ^{13}C NMR ($CDCl_3$, δ, ppm): 19.21 (t), 27.29 (t), 27.56 (t), 50.15 (q), 74.49 (s), 107.22 (s). ^{29}Si NMR ($CDCl_3$, δ, ppm): −69.23. Mass spectrum (EI; *m/e*, relative intensity): 360 (1, M^+). Elemental analyses calculated for $C_{15}H_{28}O6Si_2$: C, 49.97; H, 7.83. Found: C, 47.63; H, 7.55.

1,10-Bis(trimethoxysil)-1,9-decadiyne, P_6. Experimental procedure similar to the preparation of **P_2**. The following quantities were used: 1,9-decadiyne (11.6 g, 86.4 mmol) in tetrahydrofurane (350 mL); solution of MeLi/LiBr in ether (130 mL, [MeLi] = 1.5 M); chlorotrimethoxysilane (32.5 g, 207.6 mmol) in 100 mL of THF. Distillation (149−154 °C, 2×10^{-2} mmHg) gave 25.1 g (yield, 78%) of a pale yellow liquid. IR (CCl_4, ν cm^{-1}): 1090, 1428, 1463, 2185, 2843, 2942. ^{1}H NMR (CCl_4, δ, ppm): 1.24 (8H, m), 2.02 (4H, t), 3.26 (18H, s). ^{13}C NMR ($CDCl_3$, δ, ppm): 19.30 (t), 27.76 (t), 27.83 (t), 50.48 (q), 74.57 (s), 107.78 (s). ^{29}Si NMR ($CDCl_3$, δ, ppm): −69.22. Mass spectrum (EI; *m/e*, relative intensity); 374 (1, M^+). Elemental analyses calculated for $C_{16}H_{30}O6Si_2$: C, 51.30; H, 8.07. Found: C, 50.09; H, 8.14.

1,12-Bis(trimethoxysil)-1,11-dodecadiyne, P_8. An experimental procedure similar to that used for the preparation of **P_2** was used. The following quantities were used: 1,11-dodecadiyne (12.9 g, 79.5 mmol) in tetrahydrofurane (350 mL); solution of MeLi/LiBr in ether (120 mL, [MeLi] = 1.5 M); chlorotrimethoxysilane (29.9 g, 191.0 mmol) in 100 mL of THF. Distillation (170−175 °C, 2×10^{-3} mmHg) gave 18.8 g (yield, 18.8%) of a pale yellow liquid. IR (CCl_4, ν cm^{-1}): 1086, 1429, 1462, 2185, 2845, 2940. ^{1}H NMR (CCl_4, δ, ppm): 1.16 (12H, m), 2.03 (4H, t), 3.32 (18H, s). ^{13}C NMR ($CDCl_3$, δ, ppm): 19.06 (t), 27.89 (t), 28.28 (t), 28.49 (t), 50.12 (q), 74.31 (s), 107.64 (s). ^{29}Si NMR ($CDCl_3$, δ, ppm): −69.10. Mass spectrum (EI; *m/e*, relative intensity); 402 (1, M^+). Elemental analyses calculated for $C_{18}H_{3034}O6Si_2$: C, 53.70; H, 8.51. Found: C, 53.71; H, 8.37.

H_2 Prepared by Hydrolysis of P_2. In a Schlenk tube, compound **P_2** (23.60 g, 74.1 mmol) in 20.7 mL of THF is mixed with distilled water (4.0 mL, 222.3 mmol, 3 mol equiv). The homogeneous solution is allowed to stand at 20 °C and a monolithic transparent pale yellow gel is formed within 6−10 s. After aging at 20 °C for 1 week, the gel is powdered, washed with ether, filtered, and dried in a vacuum at room temperature over 24 h, yielding 15.57 g of gel **H_2** as a pale yellow powder. IR (KBr, ν cm^{-1}): 1069, 1425, 2192, 2856, 2976, 3461. CP TOSS ^{13}C NMR (700 scans, δ, ppm): 19.1, 50.5, 79.9, 105.3. ^{29}Si NMR CP MAS (δ, ppm): −79.2, −88.2, −98.5. Elemental analyses calculated for $C_6H_4O_3Si_2$: C, 39.98; H, 2.24; Si, 31.16. Found: C, 35.41; H, 4.01; Si, 26.40. BET surface area: 360 m^2 g^{-1}

H_3 Prepared by Hydrolysis P_3. H_3 was prepared as outlined above using compound **P_3** (13.93 g, 41.9 mmol) in THF (11.7 mL) and distilled water (2.26 mL, 127.5 mmol); the gelation time is 140 s. Mass of **H_3** obtained is 9.04 g. IR (KBr, ν cm^{-1}): 1066, 1431, 1453, 2192, 2867, 2943, 3472. CP TOSS ^{13}C NMR (1200 scans, δ, ppm): 19.1, 28.1, 51.4, 79.1, 107.3. ^{29}Si NMR CP MAS (δ, ppm): −78.6, −87.6, −96.1. Elemental analyses calculated for $C_7H_6O_3Si_2$: C, 43.27; H, 3.11; Si, 28.91. Found: C, 41.22; H, 4.06; Si, 26.65. BET surface area: 1 m^2 g^{-1}

H_4 Prepared by Hydrolysis of P_4. H_4 was prepared as outlined above using compound **P_4** (23.11 g, 66.8 mmol) in THF

(18.65 mL) and distilled water (3.61 mL, 200.4 mmol); gelation time is 140 s. Mass of **H_4** obtained is 15.32 g. IR (KBr, ν cm^{-1}): 1060, 1431, 1458, 2192, 2867, 2943, 3446. CP TOSS ^{13}C NMR (12 000 scans, δ, ppm): 19.6, 27.6, 51.1, 78.4, 107.2. ^{29}Si NMR CP MAS (δ, ppm): −79, −87.7, −97.0. Elemental analyses calculated for $C_8H_8O_3Si_2$: C 46.13; H, 3.87; Si, 26.96. Found: C, 44.52; H, 4.72; Si, 23.95. BET surface area: 6 m^2 g^{-1}.

H_5 Prepared by Hydrolysis of P_5. H_5 was prepared as outlined above using compound **P_5** (21.17 g, 58.7 mmol) in THF (16.40 mL) and distilled water (3.17 mL, 176.1 mmol); gelation time is 30 s. Mass obtained of **H_5** is 14.20 g. IR (KBr, ν cm^{-1}): 1075, 1425, 1458, 2191, 2867, 2943, 3442. CP TOSS ^{13}C NMR (2900 scans, δ, ppm): 20.0, 26.9, 50.8, 78.6, 107.2. ^{29}Si NMR CP MAS (δ, ppm): −79, −87.8, −96.7. Elemental analyses calculated for $C_9H_{10}O_3Si_2$: C, 48.62; H, 4.53; Si, 25.26. Found: C, 47.47; H, 5.38; Si, 24.00. BET surface area: <5 m^2 g^{-1}.

H_6 Prepared by Hydrolysis of P_6. H_6 was prepared as outlined above using compound **P_6** (20.42 g, 54.5 mmol) in THF (15.23 mL) and distilled water (2.94 mL, 163.5 mmol); gelation time is 35 s. Mass of **H_6** obtained is 13.45 g. IR (KBr, ν cm^{-1}): 1099, 1425, 1458, 2192, 2856, 2932, 3432. CP TOSS ^{13}C NMR (17 000 scans, δ, ppm): 20.0, 28.3, 50.8, 78.6, 107.2. ^{29}Si NMR CP MAS (δ, ppm): −87.3, −96.0. BET surface area: <5 m^2 g^{-1}.

H_8 Prepared by Hydrolysis of P_8. H_8 was prepared as outlined above using compound **P_8** (28.60 g, 71.0 mmol) in THF (19.84 mL) and distilled water (3.83 mL, 213.0 mmol); gelation time is 10 s. Mass of **H_8** obtained is 20.21 g. IR (KBr, ν cm^{-1}): 1118, 1425, 1458, 2191, 2856, 2934, 3444. CP TOSS ^{13}C NMR (3500 scans, δ, ppm): 20.1, 28.4, 50.8, 78.1, 106.8. ^{29}Si NMR CP MAS (δ, ppm): −86.6, −97.1. Elemental analyses calculated for $C_{12}H_{16}O_3Si_2$: C, 54.51; H, 6.10; Si, 21.24. Found: C, 54.20; H, 6.92; Si, 20.50. BET surface area: <5 m^2 g^{-1}.

Preparation of T_4. Calcination of **H_4** (3.96 g) in dried air (flow of 50 mL min^{-1}) at 680 °C for 4 h gives **T_4** as a white powder (2.06 g). IR (KBr, ν cm^{-1}): 1082, 3451. ^{29}Si NMR CP MAS (δ, ppm): −107.7. Elemental analyses: C, 0.26; H, 0.51; Si, 44.70. BET surface area: 345 m^2 g^{-1}. Pore volume: 0.17 cm^3 g^{-1}. Average pore diameter: 14.6.Å.

Preparation of T_8 Calcination of **H_8** (3.96 g) under a dried air flow at 600 °C for 4 h gives **T_8** as a white powder (2.06 g). IR (KBr, ν cm^{-1}): 1085, 3455. ^{29}Si NMR CP MAS (δ, ppm): −107.5. Elemental analyses: C, 0.20; H, 0.42; Si, 45.1. BET surface area: 95 m^2 g^{-1}. Pore volume: 0.17 cm^3 g^{-1}. Average pore diameter: 14.6 Å.

Preparation of C_2 by Chemical Treatment of H_2. To **H_2** (8.69 g, 41.8 mmol) are added distilled water (90 mL), methanol (60 mL), and an aqueous solution of NH_4F (0.96 mL, [NH_4F] = 1 M). The reactive medium is refluxed and stirred over 4 days. The resulting solid is washed with THF, acetone, and ether, filtered, and dried in a vacuum at room temperature over 24 h, yielding 6.51 g of **C_2** as an ivory solid. IR (KBr, v cm^{-1}): 1086, 2218, 2191, 2856, 2976, 3303, 3446. ^{13}C NMR CP TOSS (48 000 scans, δ, ppm): 18.0, 51.7, 78.0, 82.4, 105.6. ^{29}Si NMR CP MAS (δ, ppm): −80.1, −90.9, −100.9, 110.9. Elemental analyses: C, 12.45; H, 2.44; Si, 33.15; O, 46.00; corresponding to $C_{0.88}H_{2.05}O_{2.44}Si$. BET surface area: 935 m^2 g^{-1}. Pore volume: 0.64 cm^3 g^{-1}. Average pore diameter: 27.6 Å.

Preparation of C_3 by Chemical Treatment of H_3. C_3 was prepared as outlined above using **H_3** (7.02 g, 36.1 mmol), distilled water (80 mL), methanol (60 mL), and an aqueous solution of NH_4F (0.72 mL, [NH_4F] = 1 M), yielding 4.44 g of **C_3** as an ivory solid. IR (KBr, ν cm^{-1}): 1078, 2118, 2191, 2856, 2965, 3292, 3441. ^{29}Si NMR CP MAS (δ, ppm): −92.4, −100.9, −110.2. Elemental analyses: C, 6.83; H, 1.63; Si, 40.60; O, 50.77; corresponding to $C_{0.39}H_{1.12}O_{2.19}Si$. BET surface area: 684 m^2 g^{-1}. Pore volume: 0.88 cm^3 g^{-1}. Average pore diameter: 51.3 Å.

Preparation of C_4 by Chemical Treatment of H_4. C_4 was prepared as outlined above using **H_4** (8.50 g, 40.9 mmol), distilled water (80 mL), methanol (40 mL), and an aqueous solution of NH_4F (0.82 mL, [NH_4F] = 1 M), yielding 4.84 g of **C_4** as an ivory solid. IR (KBr, ν cm^{-1}): 1090, 2191, 2856, 2965, 3464. ^{13}C NMR CP TOSS (34 000 scans, δ, ppm): 17.7, 27.2, 50.5, 77.4, 84.9, 107.0. ^{29}Si NMR CP MAS (δ, ppm): −92.0, −100.8, −111.8. Elemental analyses: C, 5.72; H, 1.36; Si, 40.90; O, 51.50; corresponding to $C_{0.33}H_{0.93}O_{2.21}Si$. BET surface area: 441 m^2 g^{-1}. Pore volume: 0.78 cm^3 g^{-1}. Average pore diameter: 70.4 Å.

Preparation of C_5 by Chemical Treatment of H_5. C_5 was prepared as outlined above using **H_5** (7.01 g, 31.5 mmol), distilled water (70 mL), methanol (60 mL), and an aqueous solution of NH_4F (0.63 mL, [NH_4F] = 1 M), yielding 4.77 g of **C_5** as an ivory solid. IR (KBr, ν cm^{-1}): 1097, 1431, 1464, 2194, 2867, 2943, 3303, 3455. ^{13}C NMR CP TOSS (3200 scans, δ, ppm): 19.4, 28.2, 51.5, 78.1, 84.7, 106.5. ^{29}Si NMR CP MAS (δ, ppm): −88.7, −99.7, −109.8. Elemental analyses: C, 23.46; H, 3.03; Si, 33.05; O, 38.93; corresponding to $C_{1.66}H_{2.55}O_{2.07}Si$. BET surface area: 383 m^2 g^{-1}. Pore volume: 0.36 cm^3 g^{-1}. Average pore diameter: 38.0 Å.

Preparation of C_6 by Chemical Treatment of H_6. C_6 was prepared as outlined above using **H_6** (10.05 g, 42.5 mmol), distilled water (90 mL), methanol (60 mL), and an aqueous solution of NH_4F (0.85 mL, [NH_4F] = 1 M), yielding 8.23 g of **C_6** as an ivory solid. IR (KBr, ν cm^{-1}): 1102, 1425, 1464, 2194, 2856, 2952, 3292, 3451. ^{13}C NMR CP TOSS (13 000 scans, δ, ppm): 19.9, 28.7, 51.0, 78.0, 85.3, 107.1. ^{29}Si NMR CP MAS (δ, ppm): −87.5, −97.8, −109.6. Elemental analyses: C, 40.30; H, 4.52; Si, 25.60; O, 29.58; corresponding to $C_{3.68}H_{4.92}O_{2.03}Si$. BET surface area: 58 m^2 g^{-1}. Pore volume: 0.09 cm^3 g^{-1}. Average pore diameter: 62.2 Å.

Preparation of C_8 by Chemical Treatment of H_8. C_8 was prepared as outlined above using **H_8** (13.10 g, 49.5 mmol), distilled water (100 mL), methanol (50 mL), and an aqueous solution of NH_4F (0.99 mL, [NH_4F] = 1 M), yielding 12.59 g of **C_8** as an ivory solid. IR (KBr, ν cm^{-1}): 1108, 1431, 1464, 2193, 2856, 2939, 3433. ^{13}C NMR CP TOSS (20 000 scans, δ, ppm): 19.9, 28.4, 50.7, 77.5, 106.5, 107.1. ^{29}Si NMR CP MAS (δ, ppm): −76.3, −88.1, −97.6, −108.6. Elemental analyses: C, 53.53; H, 6.50; Si, 21.75; O, 18.22; corresponding to $C_{5.75}H_{8.33}O_{1.47}Si$. BET surface area: <5 m^2 g^{-1}.

Preparation of CT_2. Calcination of the silica **C_2** (3.19 g) in dried air flow (50 mL min^{-1}) at 600 °C for 4 h gives **CT_2** as a white powder (2.47 g). IR (KBr, ν cm^{-1}): 1090, 3446. ^{29}Si NMR CP MAS (δ, ppm): −90.4, −99.5, −107.5. Elemental analyses: C, 1.03; H, 0.41; Si, 40.00; corresponding to $C_{0.06}H_{0.29}O_{2.36}Si$. BET surface area: 780 m^2 g^{-1}. Pore volume: 0.48 cm^3 g^{-1}. Average pore diameter: 24.8 Å.

Preparation of CT_3. CT_3 was prepared as outlined above using **C_3** (3.05 g) to give a white powder (2.61 g). IR (KBr, ν cm^{-1}): 1085, 3450. ^{29}Si NMR CP MAS (δ, ppm): −109.7. Elemental analyses: calculated Si 46.74; experimental C 0.53; H, 0.51; Si, 43.85; corresponding to $C_{0.03}H_{0.32}O_{2.23}Si$. BET surface area: 685 m^2 g^{-1}. Pore volume: 0.85 cm^3 g^{-1}. Average pore diameter: 49.5 Å.

Preparation of CT_4. CT_4 was prepared as outlined above using **C_4** (2.25 g) to give a white powder (2.01 g). IR (KBr, ν cm^{-1}): 1094, 3457. ^{29}Si NMR CP MAS (δ, ppm): −108.0. Elemental analyses: C, 0.20; H, 0.32; Si, 44.90; corresponding to $C_{0.01}H_{0.20}O_{2.03}Si$. BET surface area: 407 m^2 g^{-1}. Pore volume: 0.72 cm^3 g^{-1}. Average pore diameter: 70.5 Å.

Preparation of CT_5. CT_5 was prepared as outlined above using silica **C_5** (2.82 g) to give a white powder (1.98 g). IR (KBr, ν cm^{-1}): 1094, 3450. ^{29}Si NMR CP MAS (δ, ppm): −107.6. Elemental analyses: C, 0.48; H, 0.46; Si, 45.75; corresponding to $C_{0.02}H_{0.28}O_{2.05}Si$. BET surface area: 546 m^2 g^{-1}. Pore volume: 0.59 cm^3 g^{-1}. Average pore diameter: 43.1 Å.

Preparation of CT_6. CT_6 was prepared as outlined above using **C_6** (3.68 g) to give a white powder (2.03 g). IR (KBr, ν cm^{-1}): 1098, 3444. ^{29}Si NMR CP MAS (δ, ppm): −100.7. Elemental analyses: C, 0.3; H, 0.33; Si, 42.0; corresponding to $C_{0.02}H_{0.22}O_{2.31}Si$. BET surface area: 329 m^2 g^{-1}. Pore volume: 0.20 cm^3 g^{-1}. Average pore diameter: 24.9 Å.

Preparation of CT_8. CT_8 was prepared as outlined above using **C_8** (4.15 g) to give a white powder (1.71 g). IR (KBr, ν cm^{-1}): 1094, 3444. ^{29}Si NMR CP MAS (δ, ppm): −101.3. BET surface area: 298 m^2 g^{-1}. Pore volume: 0.13 cm^3 g^{-1}. Average pore diameter: 15.1 Å.

CM980519I